JOURNAL OF GUIDANCE, CONTROL, AND DYNAMICS
Vol. 18, No. 2, March–April 1995

Robust Roll Modulation Guidance for Aeroassisted Mars Mission

Nick A. Thorp* and Bion L. Pierson†
Iowa State University, Ames, Iowa 50011-3231

The utility of using an aggregate measure of a vehicle's performance in determining the gains in a fixed-structure guidance scheme for an aeromaneuvering spacecraft so as to increase the "robustness" of the vehicle's performance is examined. The gains in the guidance scheme are determined by minimizing an "averaged" performance measure based upon the vehicle's flight through several different atmosphere models. This technique is applied to a Martian aeromaneuvering problem. Simulation results using gains determined by this method show a significant increase in off-nominal performance.

Nomenclature

A = amplitude of the sine wave
C_D = vehicle's coefficient of drag
C_L = vehicle's coefficient of lift
g = local gravitational acceleration
h = altitude rate
$\dot{h}_{\text{ref}}$ = reference altitude rate
h_{ref} = reference altitude
$\boldsymbol{h}_{\text{actual}}$ = angular momentum vector of the actual orbit
$\boldsymbol{h}_{\text{target}}$ = angular momentum vector of the target orbit
m = vehicle's mass
n = number of different atmospheres
$\bar{q}$ = dynamic pressure
$\bar{q}_{\text{ref}}$ = reference dynamic pressure
R = planetary radius
r = radial distance to vehicle
r_{a,exit_i} = radial apoapsis distance based on flight conditions at atmospheric exit after flight through ith atmosphere
$r_{a,\text{target}}$ = specified radial apoapsis distance of target orbit
r_{p,exit_i} = radial periapsis distance based on flight conditions at atmospheric exit after flight through ith atmosphere
$r_{p,\text{target}}$ = specified radial periapsis distance of target orbit
S = vehicle's aerodynamic reference area
V = vehicle's velocity
V_{trigger} = threshold velocity for guidance scheme switching
W = weight of the vehicle
γ = vehicle's flight-path angle
ΔV_{1i} = ΔV at actual apoapsis required to adjust actual periapsis to targeted periapsis after flight through ith atmosphere
ΔV_{2i} = ΔV at actual periapsis required to adjust actual apoapsis to targeted apoapsis after flight through ith atmosphere
ΔV_{3i} = ΔV required to adjust orientation of orbit, i.e., to align actual orbit's momentum vector with targeted orbit's momentum after flight through ith atmosphere
δ = bias
ζ = damping factor for roll model
θ = longitude of vehicle
μ = Martian gravitational parameter
ρ = atmospheric density
ρ_{nominal} = atmospheric density from the nominal atmosphere model at an altitude of h
σ = vehicle's bank angle
σ_c = commanded bank angle from guidance system
ϕ = latitude of vehicle
ϕ_{atm} = phase angle
ψ = vehicle's heading angle
ω_n = natural frequency for roll model
$\tilde{\omega}_{\text{exit}_i}$ = "wedge angle" between actual orbit's angular momentum vector and target orbit's angular momentum vector after flight through ith atmosphere

Received March 1, 1993; presented as Paper 93-716 at the AAS/AIAA Astrodynamic Specialist Conference, Victoria, B.C., Canada, Aug. 16–19, 1993; revision received Jan. 26, 1994; accepted for publication May 2, 1994.

*Doctoral Candidate, Department of Aerospace Engineering and Engineering Mechanics. Member AIAA.
†Professor, Department of Aerospace Engineering and Engineering Mechanics. Associate Fellow AIAA.

Introduction

WHENEVER an aeroassisted mission is being planned, there will always be imprecise knowledge of the target planet atmospheric properties, the spacecraft aerodynamic characteristics, and the atmospheric entry orientation. Thus, the spacecraft guidance system must be able to compensate for these uncertainties. Several guidance schemes for aeromaneuvering flight have been presented. These strategies utilize drag coefficient modulation, lift coefficient (angle-of-attack) modulation, and/or bank angle modulation (roll about the velocity vector) as the controlling mechanism.

In the area of drag modulation, Kechichian et al.[1] have presented two guidance schemes using drag modulation for planar, nonlifting, aeroassisted flight. These strategies utilize switching between maximum and minimum C_D values and have been applied to simulated GEO-to-LEO missions, where GEO and LEO refer to geostationary Earth orbit and low Earth orbit, respectively. A related guidance scheme has been proposed by Vinh et al.[2] This scheme is less sensitive to the timing of the switching from the entry guidance phase to the exit phase. In this two-phase scheme, a constant drag coefficient is used for the initial portion of the atmospheric flight. After passing the minimum altitude point, the drag coefficient is varied to achieve a desired exit velocity. This strategy has been applied to several simulated GEO-to-LEO transfers.

In the area of lift coefficient or angle-of-attack modulation for planar, aeroassisted orbital transfer, Miele and Wang[3] have developed a feedback control scheme that adjusts the lift coefficient via a two-stage gamma (flight-path angle) guidance law. The algorithm uses the equilibrium glide lift coefficient with feedback of the error from a reference flight-path angle. This reference flight-path angle is linear with altitude during the entry portion of the aeromaneuvering flight and constant during the exit portion. This modified gamma guidance law has been successfully demonstrated on several HEO-to-LEO missions, where HEO refers to high Earth orbit. Lee and Grantham[4] have presented a guidance scheme that is based on a Lyapunov optimal function minimizing feedback control algorithm and has been successfully applied to HEO-to-LEO transfer.

Extensive use has been made of bank angle modulation for trajectory control. Hill[5] presented a fixed-structure, three-phase adaptive guidance scheme using roll about the velocity vector to modulate the lift vector for an aeromaneuvering orbital transfer vehicle. This scheme attempts to follow an equilibrium glide trajectory during the first phase of flight and then to follow reference drag and

altitude rate profiles during the last guidance phase. Roll reversals are used to maintain lateral control of the vehicle. Hill[5] and Cerimele et al.[6] apply this algorithm to several HEO-to-LEO missions. Another fixed-structure guidance scheme that uses bank angle for L/D modulation was introduced by Gamble et al.[7] This scheme has two longitudinal control phases (equilibrium glide in the entry phase and full lift-up in the exit phase) to determine the magnitude of the commanded bank angle. The lateral guidance determines the sign of the bank angle to reach a specified exit state. This algorithm was applied to a simulated GEO-to-LEO Shuttle rendezvous mission. An improved version of this guidance scheme is due to Cerimele and Gamble.[8] The two phases of longitudinal control are an equilibrium glide with feedback of altitude rate error and dynamic pressure error for the entry portion of the flight and a predictor/corrector algorithm for targeting the proper exit state in the exit portion of the flight. This guidance scheme has been successfully applied to a simulated GEO-to-LEO transfer. This scheme is used by Fitzgerald and Ward[9] in their GEO-to-LEO mission analysis, and Meyerson and Cerimele[10] have applied it to a Mars mission. Also, Gamble et al.[11] have included this scheme in their work on guidance schemes for the aeroassist flight experiment (AFE). Two other guidance algorithms (numeric predictor/corrector and energy controller) have been developed in this work. Dukeman[12] outlines two possible guidance schemes (reference apogee method and a different numeric predictor/corrector) for the AFE. Bank angle modulation has been employed in all five of these schemes, which have been demonstrated on simulated AFE flights. Braun and Powell[13] have developed a three-phase, three-degree-of-freedom, predictor-corrector, guidance algorithm. The first phase uses a constant commanded bank angle calculated to yield the proper exit energy. The second phase (load relief) is a lift vector up flight that is used only if the deceleration level is excessive. The third phase uses a constant commanded bank angle to achieve the required exit energy. Roll reversals are used during this exit phase to maintain the proper orbital plane. Powell and Braun[14] have improved the load-relief logic and the accuracy of the exit energy predictions in this guidance algorithm. This guidance scheme has been successfully demonstrated on a simulated Mars aerocapture mission. A three-phase guidance law for planar aeroassisted flight, based on the use of an approximate, analytical solution (by matched asymptotic expansions) to the planar equations of motion, has been outlined by Mease and McCreary.[15] This law, which employs bank angle modulation, consists of entry, constant altitude, and exit phases and has been applied to a simulated Martian aerocapture maneuver.

In a series of articles, Hull and his associates[16–19] have developed a minimum-energy-loss guidance law for an aeroassisted plane change maneuver between circular LEOs with the same altitude. This guidance law repetitively uses an approximate optimal control law to determine the appropriate angle of attack and bank angle. McEneaney[20] has extended this work and developed three related guidance algorithms for Earth-based plane change maneuvers.

Our intent is to increase the robustness of one of these guidance schemes for use on a Mars mission. Since atmospheric uncertainties are the primary concern, the adjustable parameters of a particular guidance scheme can be chosen to optimize a measure of mission performance in the presence of more than one model atmosphere. There is an extensive body of work in the general area of robust controller design. Dorato[21] and Dorato and Yedavalli [22] have compiled and edited two volumes of selected recent conference papers that provide an excellent survey of controller design methods that may be used to decrease sensitivity. Most of these techniques, however, are restricted to systems with linear dynamics. Two concepts from robust controller design seem applicable to our problem. A minimax method of controller design that gives the best linear-quadratic-Gaussian closed-loop performance over a set of worst plant parameter changes has been presented by Mills and Bryson.[23] Since they have linear dynamics, the evaluation of the worst plant parameter changes is analytic. To extend this concept to nonlinear dynamics would require extensive computation. Also, Ray and Stengel[24] have developed a method of stochastic robustness analysis that could be used in the development of a robust flight controller. This analysis approach has been applied to nonlinear systems. Again, an intensive computational effort would be required to determine an optimal fixed-structure controller based on minimizing a probability from the stochastic robustness analysis. Consequently, to reduce the required computational burden, we propose to determine the gains in a fixed-structure guidance scheme by minimizing an "averaged" performance measure based upon the vehicle's flight through several representative atmosphere models.

To investigate the utility of this technique, a hypothetical aeroassisted Mars mission is examined. In this mission, the spacecraft's physical description, position, velocity, and orientation are known when the vehicle first encounters the Martian atmosphere. A single aeroassisted pass through the Martian atmosphere is used for the aerocapture of the spacecraft. During this atmospheric pass, bank angle modulation is used to control the trajectory. This type of flight control produces a nonplanar trajectory rather than the planar trajectory produced by a drag modulation control scheme. Upon exiting from the Martian atmosphere, the spacecraft uses three impulsive engine burns to enter a specified elliptic orbit about Mars. In order, these ΔV adjust the orbital 1) periapsis, 2) apoapsis, and 3) inclination and longitude of the ascending node to the prescribed target orbit values.

Problem Statement

The general problem then is to determine the values of the guidance parameters (gains) in a fixed-structure guidance scheme for aeroassisted flight that will minimize some aggregate measure of the vehicle's performance when that vehicle is flown through several different atmospheres that characterize the anticipated range of atmospheres.

Equations of Motion

For the aeroassisted maneuver, it is assumed that the vehicle is flying through a nonrotating atmosphere about a nonrotating spherical planet with an inverse-square gravity field. Furthermore, it is assumed that the vehicle is flying at a constant angle-of-attack, that C_L and C_D are constant, and that the vehicle roll dynamics may be modeled as a second-order system. The equations of motion for a four-degree-of-freedom (4-DOF) system (three-dimensional translational equations plus roll dynamics) are employed so that the selected guidance scheme may use logic for both longitudinal and lateral maneuvers in attempting to meet the specified atmospheric exit conditions. These 4-DOF equations of motion, which contain the commanded bank angle σ_c as the only control function, are given by[25]

$$\begin{aligned}
\dot{r} &= V\sin\gamma \\
\dot{\theta} &= \frac{V\cos\gamma\cos\psi}{r\cos\phi} \\
\dot{\phi} &= \frac{V\cos\gamma\sin\psi}{r} \\
\dot{V} &= \frac{-C_D S}{2m}\rho V^2 - \frac{\mu}{r^2}\sin\gamma \\
\dot{\gamma} &= \frac{C_L S}{2m}\rho V\cos\sigma + \left(\frac{V}{r} - \frac{\mu}{r^2 V}\right)\cos\gamma \\
\dot{\psi} &= \frac{C_L S}{2m}\rho V\frac{\sin\sigma}{\cos\gamma} - \frac{V}{r}\cos\gamma\cos\psi\tan\phi \\
\ddot{\sigma} &= -2\zeta\omega_n\dot{\sigma} - \omega_n^2(\sigma - \sigma_c)
\end{aligned} \tag{1}$$

Performance Indices

There are several possible objective functions that could be used to measure the overall performance of the vehicle as it is flown through several different Martian atmospheres. Since the main motivation for an aeroassisted maneuver is to save fuel,[26,27] i.e., total ΔV, the average total ΔV could be used as a measure of the vehicle's performance,

$$J_1 = \frac{\sum_{i=1}^{n}(|\Delta V_{1_i}| + |\Delta V_{2_i}| + |\Delta V_{3_i}|)}{n} \tag{2}$$

The equations for the calculation of the ΔV in this performance index are shown in the Appendix.

Alternately, the average total deviation of the actual orbit, before ΔV corrections are applied, from the target orbit parameters could be employed as a performance index,

$$J_2 = \frac{\sum_{i=1}^{n}(|r_{a,\text{exit}_i} - r_{a,\text{target}}| + |r_{p,\text{exit}_i} - r_{p,\text{target}}| + |\tilde{\omega}_{\text{exit}_i}|)}{n} \tag{3}$$

Potential scaling problems with this performance measure are avoided since all of the actual computations involve normalized variables.

Guidance Algorithm

Several of the possible guidance algorithms for aeroassisted flight that could be used in this study have been mentioned in the Introduction. The only restriction on the guidance scheme for this study is that the scheme be of a fixed structure with selectable gains.

Many of the guidance algorithms for aeroassisted maneuvers, including the algorithm used in this study, are discrete in nature. Here, a discrete guidance scheme is a guidance algorithm that will issue new guidance commands at discrete, periodic times. Thus, a guidance command is applied for a fixed, finite-length time interval ($\Delta T_{\text{guidance-cycle}}$), and it is assumed that there is no time delay in the computation of a guidance command.

Each of these discrete guidance schemes meets the fixed-structure requirement. For this study, the analytic predictor/corrector guidance scheme of Gamble et al.[11] will be used, with minor modifications in the lateral guidance algorithm due to Dukeman.[12] This is a fixed-structure guidance scheme with G_ρ, $G_{\dot{q}}$, $G_{\dot{h},\text{entry}}$, $G_{\dot{h},\text{exit}}$, V_{scale}, and W_{slope} as design parameters. This guidance algorithm may be summarized as follows.[11]

At the start of each guidance cycle, C_D, S, m, the spacecraft's current state (h, θ, ϕ, V, γ, ψ), and the drag acceleration $\dot{V}$ must be available for guidance computations. In flight, the spacecraft's current state and drag acceleration will be available from measurements. First, determine the density from the drag acceleration,

$$\rho_d = 2\dot{V}m/(C_D S V^2) \tag{4}$$

Then, compute the filtered density multiplier for the next guidance cycle ($K_{\rho_{i+1}}$),

$$K_{\rho_{i+1}} = (1 - G_\rho)K_{\rho_i} + G_\rho(\rho_d/\rho_{\text{nominal}}) \tag{5}$$

The density value used in the remaining guidance calculations may be determined by

$$\rho_{\text{guidance}} = K_{\rho_{i+1}}\rho_{\text{nominal}} \tag{6}$$

The magnitude of the commanded bank angle is determined so that the apoapsis distance based on the flight conditions at atmospheric exit is as close as possible to the targeted apoapsis distance. For the entry portion of the flight (when $V > V_{\text{trigger}}$),

$$\cos\sigma_c = \frac{1}{\bar{q}}\left(\frac{W(1 - V^2/gR)}{C_L S} - G_{\dot{h}}\dot{h} + G_{\bar{q}}(\bar{q} - \bar{q}_{\text{ref}})\right) \tag{7}$$

For the exit portion of the flight (when $V \le V_{\text{trigger}}$),

$$\cos\sigma_c = \frac{1}{\bar{q}}\left(\frac{W(1 - V^2/gR)}{C_L S} - G_{\dot{h}}(\dot{h} - \dot{h}_{\text{ref}})\right) \tag{8}$$

The lateral guidance scheme (determining the sign of the commanded bank angle) tries to establish and to maintain the vehicle's position and velocity vectors in the targeted orbital plane. The wedge angle ($\tilde{\omega}$) between the angular momentum vectors for the targeted orbital plane and the orbital plane based on the current conditions is a measure of the success of this attempted alignment. Thus, the lateral guidance scheme attempts to maintain $\tilde{\omega}$ at 0 deg. The initial deviations of position and velocity from the specified orbital plane are assumed to be small. Thus, the lateral portion of the guidance scheme is as follows.

The commanded bank angle's sign is determined by evaluating the current wedge angle,

$$\cos\tilde{\omega} = \frac{\boldsymbol{h}_{\text{actual}} \cdot \boldsymbol{h}_{\text{target}}}{|\boldsymbol{h}_{\text{actual}}||\boldsymbol{h}_{\text{target}}|} \tag{9}$$

Then, compute a maximum acceptable wedge angle,

$$\tilde{\omega}_{\max} = (V - V_{\text{scale}})W_{\text{slope}} \tag{10}$$

The appropriate sign for the commanded bank angle is then determined:

$$\text{Sign} = \begin{cases} -\text{sgn}(\boldsymbol{V}_{\text{actual}} \cdot \boldsymbol{h}_{\text{target}}) & \text{if} \quad \tilde{\omega} > \tilde{\omega}_{\max} \\ -\text{sgn}(\boldsymbol{r}_{\text{actual}} \cdot \boldsymbol{h}_{\text{target}}) & \text{if} \quad \tilde{\omega} \le \tilde{\omega}_{\max} \end{cases} \tag{11}$$

Thus, the commanded bank angle becomes

$$\sigma_c = \text{Sign}|\sigma_c| \tag{12}$$

This is the control law for the analytic predictor/corrector guidance scheme. When this control law is used in Eq. (1), the nonlinear closed-loop dynamics are obtained.

Atmosphere Models

The atmospheric models involved in this study are all based on exponential models of the Martian atmosphere[28] of the form

$$\rho = \rho_0 e^{-\beta(h - h_0)} \tag{13}$$

The nominal model for the Martian atmosphere has been taken as a two-parameter (ρ_0, β), nonlinear, least-squares fit to the Northern Hemisphere, summer data.[28] The atmospheric density from this model is used in the guidance scheme to establish a commanded bank angle.

In order to simulate variations in the Martian atmosphere, a biased sine wave, similar to that used in Ref. 13, is imposed upon the nominal model atmosphere used by the guidance system:

$$\rho = \rho_{\text{nominal}}\left[1 + \delta + A\,\sin\left(\frac{2\pi h}{h_{\text{ref}}} + \phi_{\text{atm}}\right)\right] \tag{14}$$

Each choice of the parameter vector (δ, A, h_{ref}, ϕ_{atm}) then generates a new model atmosphere.

Problem Statement

Thus, the general problem is to determine the guidance parameters G_ρ, $G_{\bar{q}}$, $G_{\dot{h},\text{entry}}$, $G_{\dot{h},\text{exit}}$, V_{scale}, and W_{slope} in the given fixed-structure guidance scheme that will minimize an aggregate performance index (2) or (3) subject to the nonlinear closed-loop dynamic equations (1) and (4–12) for a specified set of n model atmospheres.

Solution Method

Gradient-based methods, such as sequential quadratic programming or gradient restoration, are currently among the most efficient methods for solving many finite-dimensional optimization problems. These methods assume that the objective function and the gradients of the objective function and constraints are continuous. This is not the case for the problem treated here. Thus, an optimization scheme based on only function values will be employed for this problem. An algorithm for solving inequality-constrained optimization problems has been developed by Box.[29] Kuester and Mize[30] present a computer code based upon this algorithm. A modified version of this code is used in this investigation. The code modifications involve changes in the testing for feasible points, the generation of feasible points, and the generation of the initial complex. Also, a restart capability has been added to the code, and a new output format has been installed. Although not needed in the current study, the computer code's ability to handle inequality constraints will be necessary in future work.

A Martian aeromaneuvering guidance problem has been solved. There are two versions of this problem depending upon which performance index is used: average total ΔV [Eq. (2)] or average total deviation from the specified target orbit parameters [Eq. (3)]. For

this problem, a training set of model atmospheres is defined. This set of model atmospheres represents average (nominal), extreme, and/or varied atmospheres, and this set of atmospheres remains constant throughout the entire investigation of both versions of this particular problem. For a particular version of this problem, Box's COMPLEX method is used to determine the optimal set of guidance gains. For comparison purposes, a set of optimal guidance system gains based upon flight through only the nominal model atmosphere is also obtained by use of the COMPLEX method. The vehicle's performance, in terms of the required ΔV and nearness of the aerocaptured orbit to the targeted orbit, can then be compared for flight through each of the model atmospheres in the defined set using each of the two different optimal gain sets. This procedure is employed for each of the two versions of this problem.

In the simulation and optimization programs, no limits have been placed upon the roll rate and roll acceleration in the second-order model of the vehicle's roll dynamics. Also, there is no time lag associated with the calculations of the commanded bank angle. The vehicle's atmospheric trajectory is generated using a variable-stepsize fourth-order Runge–Kutta–Fehlberg integration scheme.[31]

Results

This demonstration problem uses seven different Martian model atmospheres in the performance measure. Thus, the two versions of this problem may be stated as follows. Determine the set of six guidance system gains G_ρ, $G_{\dot{q}}$, $G_{\dot{h},\text{entry}}$, $G_{\dot{h},\text{exit}}$, V_{scale}, and W_{slope} that minimizes Eq. (2) or (3) with $n = 7$ subject to the equations of motion of the vehicle [Eq. (1)] and the equations of the guidance algorithm [Eqs. (4–12)].

The spacecraft is flown through the seven different Martian model atmospheres shown in Fig. 1 and defined in Tables 1 and 2. These model atmospheres consist of a nominal atmosphere; a cool, low-pressure atmosphere; a warm, high-pressure atmosphere; and four varied atmospheres. The nominal atmosphere is the model atmosphere used by the guidance system. The cool, low-pressure atmosphere and the warm, high-pressure atmosphere represent two atmospheric extremes.[28] The four varied atmospheres are modeled, as previously mentioned, as biased sine waves imposed upon the nominal atmosphere.

The parameter values that define this problem are shown in Table 3. The gain values at the beginning of the optimization process and the optimal gain values for both versions of this problem, along with their bounding values, are shown in Table 4. Table 5

Table 1 Parameters for model exponential atmospheres

Model atmosphere	Reference altitude, km	Reference density, kg/m^3	Inverse scale height, km^{-1}
Nominal	40.0	0.00033648	0.11330
Cool, low pressure	40.0	0.00026402	0.11966
Warm, high pressure	40.0	0.00050554	0.10612

Table 2 Parameters for model varied atmospheres

Biased sine wave model	Bias	Amplitude	Reference altitude, km	Phase angle, rad
1	0.1	0.1	15	0.00
2	−0.1	0.1	15	0.00
3	0.2	0.3	10	0.00
4	−0.2	0.3	10	0.00

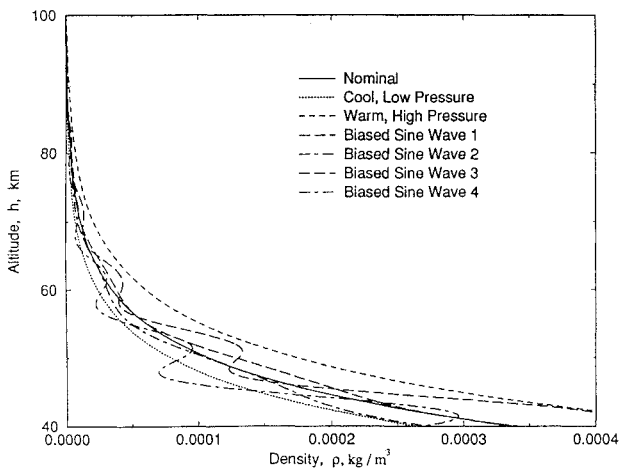

Fig. 1 Model Martian atmospheres.

Table 3 Parameters that define this Martian aeromaneuvering problem

Parameter	Definition	Value	Unit
C_L	Lift coefficient	0.618	
C_D	Drag coefficient	1.030	
h_{entry}	Atmospheric entry altitude	100.000	km
θ_{entry}	Atmospheric entry longitude	0	deg
ϕ_{entry}	Atmospheric entry latitude	0	deg
V_{entry}	Atmospheric entry velocity	6.700	km/s
γ_{entry}	Atmospheric entry flight-path angle	−12.000	deg
ψ_{entry}	Atmospheric entry heading angle	0	deg
σ_{entry}	Atmospheric entry bank angle	0	deg
ζ	Roll model damping ratio	0.950	
ω_n	Roll model natural frequency	2.000	rad/s
V_{trigger}	Guidance scheme trigger velocity	4.500	km/s
$\Delta T_{\text{guidance-cycle}}$	Guidance cycle time	1	s
Mass	Vehicle mass	9387.084	kg
Area	Vehicle reference area	200	m^2
$h_{a,\text{target}}$	Target orbit apoapsis altitude	2000	km
$h_{p,\text{target}}$	Target orbit periapsis altitude	500	km
i_{target}	Target orbit inclination	0	deg
Ω_{target}	Target orbit ascending-node longitude	0	deg
ω_{target}	Target orbit argument of periapsis	300	deg

Table 4 Initial and optimal guidance gains

Control variable	Lower bound	Initial value	Optimal gains based on Nominal atmosphere	Optimal gains based on Seven atmospheres	Upper bound
		Total ΔV performance index			
G_ρ	0	1.000	0.8539	0.7913	1.00
$G_{\dot{q}}$	0	2.000	1.2140	1.3134	25.00
$G_{\dot{h},\text{entry}}$	0	2.000	2.2837	3.2452	25.00
$G_{\dot{h},\text{exit}}$	0	2.000	2.1309	2.1295	25.00
V_{scale}	0.10	2.722	2.8307	2.4009	4.00
W_{slope}	0.01	0.108	0.0892	0.0914	0.50
		Total deviation performance index			
G_ρ	0	1.000	0.8747	0.7427	1.00
$G_{\dot{q}}$	0	2.000	1.1986	1.3086	25.00
$G_{\dot{h},\text{entry}}$	0	2.000	2.3150	3.2466	25.00
$G_{\dot{h},\text{exit}}$	0	2.000	2.3556	2.2395	25.00
V_{scale}	0.10	2.722	2.6633	2.2058	4.00
W_{slope}	0.01	0.108	0.0739	0.0776	0.50

Table 5 Performance averages for simulated flight through seven model atmospheres

Flight trajectory measure	Optimal gains based on Nominal atmosphere	Optimal gains based on Seven atmospheres	Percent reduction
	Total ΔV performance index		
ΔV, km/s	0.1141	0.1015	11.04
Miss distance, km	584.98	488.33	16.52
Wedge angle, deg	0.0589	0.0281	52.29
	Total deviation performance index		
ΔV, km/s	0.1124	0.1034	8.01
Miss distance, km	560.83	495.17	11.71
Wedge angle, deg	0.0756	0.0403	46.69

Table 6 Flight characteristics in various Martian atmospheres using gains based upon minimum average total ΔV

Flight characteristic	Initial value	Gains based on	
		Nominal atmosphere	Seven atmospheres
Nominal model			
Apoapsis altitude, km	4679.27	2006.31	1993.15
Periapsis altitude, km	26.45	47.01	19.40
Wedge angle, deg	0.0930	0.0012	0.0442
Total ΔV, km/s	0.3665	0.0943	0.1026
Flight time, s	196.19	274.92	249.58
Cool low-pressure model			
Apoapsis altitude, km	5338.90	2270.67	2007.30
Periapsis altitude, km	26.30	55.23	28.17
Wedge angle, deg	0.2329	0.0032	0.0118
Total ΔV, km/s	0.4217	0.1264	0.0991
Flight time, s	202.66	307.28	270.97
Warm high-pressure model			
Apoapsis altitude, km	3266.79	1924.88	1958.37
Periapsis altitude, km	38.63	−16.72	−1.77
Wedge angle, deg	0.2225	0.0900	0.0123
Total ΔV, km/s	0.2544	0.1230	0.1110
Flight time, s	201.12	206.96	213.18
Biased sine wave model 1			
Apoapsis altitude, km	4193.86	2068.21	2000.51
Periapsis altitude, km	31.40	50.18	37.12
Wedge angle, deg	0.3158	0.0942	0.0039
Total ΔV, km/s	0.3445	0.1060	0.0959
Flight time, s	200.18	269.21	256.30
Biased sine wave model 2			
Apoapsis altitude, km	5081.70	2265.90	2008.73
Periapsis altitude, km	21.49	54.58	42.65
Wedge angle, deg	0.0458	0.0743	0.0997
Total ΔV, km/s	0.3920	0.1292	0.1000
Flight time, s	191.87	285.58	274.90
Biased sine wave model 3			
Apoapsis altitude, km	4659.99	2048.42	2011.15
Periapsis altitude, km	23.95	36.65	25.60
Wedge angle, deg	0.3967	0.0458	0.0056
Total ΔV, km/s	0.3874	0.1042	0.0999
Flight time, s	191.84	251.17	243.91
Biased sine wave model 4			
Apoapsis altitude, km	4402.22	2129.48	2012.65
Periapsis altitude, km	34.25	42.33	19.29
Wedge angle, deg	0.2373	0.1033	0.0287
Total ΔV, km/s	0.3547	0.1160	0.1026
Flight time, s	214.83	275.69	255.18

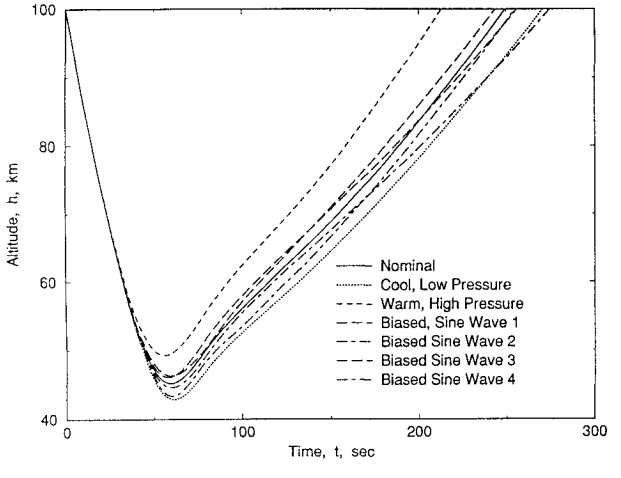

Fig. 2 Altitude time histories.

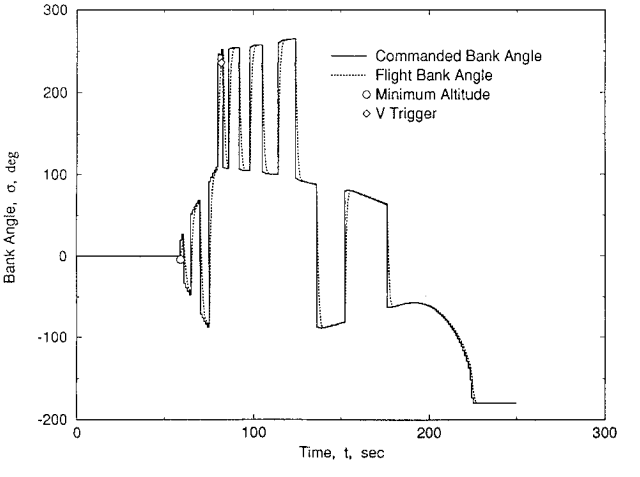

Fig. 3 Bank angle time history based upon seven-atmosphere aggregate performance index gains.

shows the average values, for flight through the seven model atmospheres, of various performance index components. Table 6 shows a summary of selected flight characteristics for trajectories using the J_1-optimal gains in each of the seven different model Martian atmospheres. Similar results were obtained using the J_2-optimal gains. Altitude time histories for flight through each of the seven model Martian atmospheres, using gains determined by minimizing the average total ΔV over seven atmospheres, are shown in Fig. 2. The bank angle time history for flight through the nominal Martian atmosphere, using gains determined by minimizing the average total ΔV over seven atmospheres, is shown in Fig. 3.

In order to observe the increase in the "robustness" of the aeromaneuvering guidance system, this same problem has been solved

Table 7 Parameters for test set of biased sine wave Martian atmospheres and ΔV performance results

Model	Bias	Amplitude	Reference altitude, km	Phase angle, deg	ΔV for gains based on: Nominal atmosphere km/s	ΔV for gains based on: Multiple (7) atmospheres, km/s
1	0.1	0.2	10	0.00	0.11229	0.10999[a]
2	0.1	0.2	10	45.00	0.10796	0.10388[a]
3	0.1	0.2	10	90.00	0.11013	0.09875[a]
4	0.1	0.2	10	−45.00	0.11263[a]	0.11871
5	0.2	0.3	7	0.00	0.10597[a]	0.11095
6	0.2	0.3	7	90.00	0.09849[a]	0.10056
7	0.2	0.3	7	180.00	0.10071[a]	0.11434
8	0.2	0.3	7	270.00	0.10183[a]	0.11404
9	−0.2	0.4	20	0.00	0.30564	0.24135[a]
10	−0.2	0.4	20	45.00	0.20203	0.18966[a]
11	−0.2	0.4	20	90.00	0.13140	0.10999[a]
12	−0.2	0.4	20	135.00	0.11137[a]	0.11321
13	−0.1	0.3	15	0.00	0.15235	0.13013[a]
14	−0.1	0.3	15	45.00	0.16028	0.11802[a]
15	−0.1	0.3	15	90.00	0.15838	0.12408[a]
16	−0.1	0.3	15	135.00	0.11052	0.10781[a]
17	0.1	0.1	15	−45.00	0.11478	0.11356[a]
18	−0.1	0.1	15	90.00	0.12510	0.09931[a]
19	0.1	0.3	10	180.00	0.10888	0.10014[a]
20	−0.1	0.3	10	90.00	0.11440	0.10914[a]
21	0.1	0.2	12	0.00	0.12301	0.10442[a]
22	0.1	0.2	12	45.00	0.10300[a]	0.10402
23	−0.2	0.1	18	−45.00	0.12325	0.09866[a]
24	−0.2	0.1	18	0.00	0.11263	0.10358[a]
Average:					0.12946	0.11826

[a]Lower ΔV value.

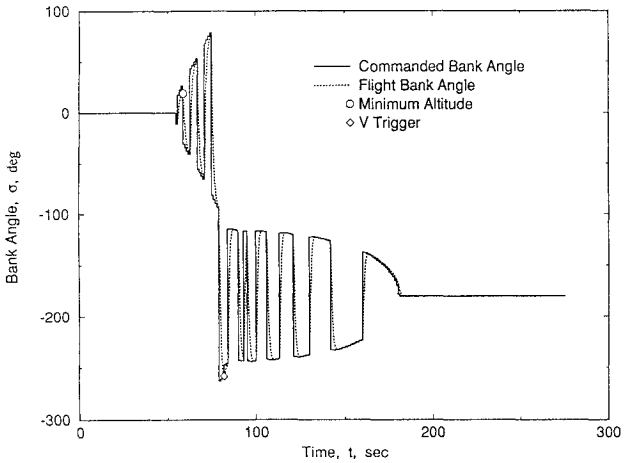

Fig. 4 Bank angle time history based upon single-atomsphere performance index gains.

using only the nominal model atmosphere; i.e., only a single atmosphere (the nominal atmosphere) is used in the performance index evaluations. These results are included in Tables 4 and 5. Also shown in Table 6 are the flight characteristics for flight through each model atmosphere using the J_1-optimal, single-atmosphere gains. Again, similar results were obtained using the J_2-optimal gains. The nominal atmosphere bank angle time history, using gains determined by minimizing the average total ΔV over a single atmosphere, is shown in Fig. 4. To further substantiate our claim of a decrease in the sensitivity of the aeromaneuvering guidance system, 24 additional biased sine wave Martian atmospheres have been defined. The parameters for these 24 atmospheres are shown in Table 7. The required ΔV for flight through each of these test atmospheres using each of the two gain sets is also recorded in Table 7.

A comparison of the flight characteristics for flight through each of the model atmospheres shows the anticipated results. Flights through the nominal model atmosphere using the optimal nominal atmosphere gains (compared to the optimal seven-atmosphere gains) have, of course, lower values for total ΔV and total deviation from the target orbit parameters. For flights through the six off-nominal model atmospheres, however, the lower values for total ΔV and for total deviation from the target orbit parameters are generally associated with the optimal seven-atmosphere gains. The superiority of the optimal seven-atmosphere gains is also shown by the various average values shown in Table 5. This table shows the average (for flight through all seven atmospheres) total ΔV, the average miss distances (the sum of the deviations from the targeted periapsis and apoapsis), and the average final wedge angles for flights using gains based on seven atmospheres and for flights using gains based only on the nominal atmosphere. In all cases, the results obtained for flight using optimal seven-atmosphere gains show a better average performance than the optimal nominal atmosphere gain based flight. The percent reduction in flight trajectory measure with respect to the nominal atmosphere gain measure is also indicated in Table 5. For example, when the guidance scheme with J_1-optimal seven-atmosphere gains is flown through each of the seven atmospheres, the average total ΔV is 0.1015 km/s, and this is an 11% improvement over using the gains optimized only over the nominal atmosphere.

The ΔV values in Table 7 indicate that the aeromaneuvering guidance scheme is more "robust" when the J_1-optimal seven-atmosphere gain set is used (compared to the J_1-optimal nominal atmosphere gain set). From the simulated flights through each of these test atmospheres, the ΔV requirement associated with the optimal seven-atmosphere gains was lower in 17 of the 24 test atmospheres. Furthermore, when the guidance scheme uses the J_1-optimal seven-atmosphere gains, the average total ΔV (for all 24 test atmospheres) is 0.11826 km/s, which is an 8.7% improvement over using the gains optimized only over the nominal atmosphere. The J_1-optimal seven-atmosphere gains also produced a 16.9% reduction in the average miss distance (from 727.2 to 604.3 m). The lower miss distance from simulated flight in 20 of the 24 test atmospheres was associated with these gains. The J_2-optimal seven-atmosphere gains also produced a more "robust" performance in simulated flights through the 24 test atmospheres. The average ΔV was reduced by 7.8% and the average miss distance was reduced by 14.0%. In these simulated flights, the seven-atmosphere-based gains produced the lower value

of the performance measure in a majority of the 24 test atmospheres. Also, Table 6 shows that the atmospheric flight times produced by guidance systems designed by aggregate seven-atmosphere performance indices are generally shorter than the flight times produced by guidance systems whose design is based upon a single model atmosphere.

The minimum altitude will change with different model atmospheres. This is reflected in the 6.42-km range in minimum altitude over the seven model atmospheres. However, the minimum altitude achieved by the vehicle in a given atmosphere is nearly the same regardless of the performance index used or the number of model atmospheres used in the gain determination. This is indicated by the small changes in minimum altitude, 0.00–0.03 km, experienced across the various performance measures in each of the different atmospheres. Consequently, the guidance system gain settings will only have a minor effect upon those quantities whose maximum value occurs near the minimum altitude point such as peak g loading, peak dynamic pressure, and peak stagnation point heating rate. Also, an examination of Fig. 2 shows that the initial plunge into the Martian atmosphere is not influenced by the type of atmosphere being encountered or by the guidance system gain settings.

Conclusions

The basic idea of this investigation is to evaluate the feasibility of determining an optimal set of gains for a discrete-time, fixed-structure guidance system based on an "averaged" performance measure for flight through multiple model atmospheres rather than flight through a single model atmosphere. The results of the investigation indicate that the vehicle's performance (measured in terms of ΔV or miss distance) using gains based upon multiple model atmospheres is superior in all of the off-nominal training atmospheres and in a majority of the other test atmospheres.

Examination of all of the simulated flight bank angle time histories reveals that roll modulation occurs over a larger portion of the atmospheric flight for guidance systems that use gains based upon an aggregate performance index. Much of the superior performance of the guidance systems using gains based upon multiple atmospheres may be attributed to this extended maneuvering period.

This guidance scheme produces a substantial number of roll reversals in order to maintain flight within the specified orbital plane. The use of gains determined by an aggregate performance index does not seem to affect the number of roll reversals.

Since the two aggregate performance indices used in this study measure a similar quantity, deviation from a specified target orbit, the two sets of optimal gains should be similar, and they are. Although the aggregate performance indices produce superior performance in off-nominal atmospheres, there does not appear to be any clear advantage to either of the two aggregate performance indices.

This approach to guidance system gain selection may be applied late in the design process after a particular guidance logic has been chosen. This investigation illustrates a practical engineering approach to making a specific guidance scheme for aeroassisted maneuvers more robust with respect to atmospheric and aerodynamic uncertainties.

Appendix: Performance Index Evaluation

At the completion of the vehicle's atmospheric flight, i.e., atmospheric exit, the spacecraft will enter an elliptical Keplerian orbit about Mars. At this atmosphere-space interface, all of the atmospheric flight trajectory variables (r_{exit}, θ, ϕ, V_{exit}, γ_{exit}, and ψ) will be known. From these known quantities, the apoapsis ($r_{a,\text{exit}}$) and periapsis ($r_{p,\text{exit}}$) of the elliptical orbit may be determined.[32] The spacecraft will follow this orbit until it reaches apoapsis. At this point the first tangential ΔV will occur. This ΔV will raise the periapsis ($r_{p,\text{exit}}$) out of the Martian atmosphere to the desired periapsis distance, $r_{p,\text{target}}$. The vehicle will then follow the new orbital path to the periapsis point. Here, the second ΔV will occur. This tangential ΔV will adjust the current apoapsis distance ($r_{a,\text{exit}}$) to the desired apoapsis distance, $r_{a,\text{target}}$. These two ΔV relations may be summarized as

$$\Delta V_1 = \sqrt{\frac{2\mu r_{p,\text{target}}}{r_{a,\text{exit}}(r_{a,\text{exit}} + r_{p,\text{target}})}} - \sqrt{V_{\text{exit}}^2 - 2\mu\frac{r_{a,\text{exit}} - r_{\text{exit}}}{r_{a,\text{exit}} r_{\text{exit}}}} \tag{A1}$$

$$\Delta V_2 = \left| \sqrt{\frac{2\mu r_{a,\text{target}}}{r_{p,\text{target}}(r_{a,\text{target}} + r_{p,\text{target}})}} - \sqrt{\frac{2\mu r_{a,\text{exit}}}{r_{p,\text{target}}(r_{a,\text{exit}} + r_{p,\text{target}})}} \right| \tag{A2}$$

The spacecraft will follow this new orbit until the third orbit adjustment point is reached. This maneuver will occur at the node line between the current orbital plane and the targeted orbital plane. Since the current orbit intersects this nodal line at two points, the fuel requirements may be minimized by executing this maneuver at the node line intersection point with the largest radial distance. The required plane rotation angle ν and ΔV for this orbital plane adjustment maneuver may be determined from the relations[33]

$$\cos\nu = \cos i_{\text{current}} \cos i_{\text{target}} + \sin i_{\text{current}} \sin i_{\text{target}} \cos(|\Omega_{\text{target}} - \Omega_{\text{current}}|) \tag{A3}$$

$$\Delta V_3 = 2V_{\text{node}} \sin(\nu/2) \tag{A4}$$

where i_{current} is the inclination of the current orbital plane, i_{target} is the inclination of the targeted orbital plane, Ω_{current} is the longitude of the ascending node of the current orbital plane, Ω_{target} is the longitude of the ascending node of the targeted orbital plane, and V_{node} is the spacecraft velocity at the node line intersection point.

Also, the wedge angle $\tilde{\omega}$, the angle between the angular momentum vectors of the targeted orbit and the orbit based on atmospheric exit conditions, may be evaluated by Eq. (9), where $\boldsymbol{h}_{\text{actual}} = \boldsymbol{r}_{\text{exit}} \times \boldsymbol{V}_{\text{exit}}$.

References

[1]Kechichian, J. A., Cruz, M. I., Rinderle, E. A., and Vinh, N. X., "Optimization and Closed-Loop Guidance of Drag-Modulated Aeroassisted Orbital Transfer," AIAA Paper 83-2093, Aug. 1983.

[2]Vinh, N. X., Johannesen, J. R., Mease, K. D., and Hanson, J. M., "Explicit Guidance of Drag Modulated Aeroassisted Transfer Between Elliptical Orbits," *Journal of Guidance, Control, and Dynamics*, Vol. 9, No. 3, 1986, pp. 274–280.

[3]Miele, A., and Wang, T., "Gamma Guidance of Trajectories for Coplanar, Aeroassisted Orbital Transfer," *Journal of Guidance, Control, and Dynamics*, Vol. 15, No. 1, 1992, pp. 255–262.

[4]Lee, B., and Grantham, W. J., "Aeroassisted Orbital Maneuvering Using Lyapunov Optimal Feedback Control," *Journal of Guidance, Control, and Dynamics*, Vol. 12, No. 2, 1989, pp. 237–242.

[5]Hill, O., "An Adaptive Guidance Logic for an Aeroassisted Orbital Transfer Vehicle," American Astronautical Society, Paper 83-357, Lake Placid, NY, Aug. 1983.

[6]Cerimele, C. J., Skalecki, L. M., and Gamble, J. D., "Meteorological Accuracy Requirements for Aerobraking Orbital Transfer Vehicles," AIAA Paper 84-0030, Jan. 1984.

[7]Gamble, J. D., Cerimele, C. J., and Spratlin, K., "Aerobraking of a Low L/D Manned Vehicle from GEO Return to Rendezvous with the Space Shuttle," AIAA Paper 83-2110, Aug. 1983.

[8]Cerimele, C. J., and Gamble, J. D., "A Simplified Guidance Algorithm for Lifting Aeroassist Orbital Transfer Vehicles," AIAA Paper 85-0348, Jan. 1985.

[9]Fitzgerald, S. M., and Ward, D. T., "Aeroassisted Orbital Transfer Vehicle Guidance Performance in the Presence of Density Dispersions," AIAA Paper 88-0302, Jan. 1988.

[10]Meyerson, R. E., and Cerimele, C. J., "Aeroassist Vehicle Requirements for a Mars Rover / Sample Return Mission," AIAA Paper 88-0303, Jan. 1988.

[11]Gamble, J. D., Cerimele, C. J., Moore, T. E., and Higgins, J., "Atmospheric Guidance Concepts for an Aeroassist Flight Experiment," *Journal of the Astronautical Sciences*, Vol. 36, No. 1/2, 1988, pp. 45–71.

[12]Dukeman, G. A., "Development of Atmospheric Guidance Schemes for the Aeroassist Flight Experiment," M. S. Thesis, Iowa State Univ., Ames, IA, 1988.

[13]Braun, R. D., and Powell, R. W., "Predictor-Corrector Guidance Algorithm for Use in High-Energy Aerobraking System Studies," *Journal of Guidance, Control, and Dynamics*, Vol. 15, No. 3, 1992, pp. 672–678.

[14]Powell, R. W., and Braun, R. D., "A Six-Degree-of-Freedom Guidance and Control Analysis of Mars Aerocapture," AIAA Paper 92-0736, Jan. 1992.

[15]Mease, K. D., and McCreary, F. A., "Atmospheric Guidance Law for Planar Skip Trajectories," AIAA Paper 85-1818, Aug. 1985.

[16]Hull, D. G., Giltner, J. M., Speyer, J. L., and Mapar, J., "Minimum Energy-Loss Guidance for Aeroassisted Orbital Plane Change," *Journal of Guidance, Control, and Dynamics*, Vol. 8, No. 4, 1985, pp. 487–493.

[17]Hull, D. G., "New Analytical Results for AOTV Guidance," *Proceedings of the 12th AIAA Atmospheric Flight Mechanics Conference*, AIAA, New York, 1985, pp. 416–420.

[18]Hull, D. G., McClendon, J. R., and Speyer, J. L., "Aeroassisted Orbital Plane Change Using an Elliptic Drag Polar," *Journal of the Astronautical Sciences*, Vol. 36, No. 1/2, 1988, pp. 73–87.

[19]Hull, D. G., McClendon, J. R., and Speyer, J. L., "Improved Aeroassisted Plane Change Using Successive Approximation," *Journal of the Astronautical Sciences*, Vol. 36, No. 1/2, 1988, pp. 89–101.

[20]McEneaney, W. M., "Optimal Aeroassisted Guidance Using Loh's Term Approximations," *Journal of Guidance, Control, and Dynamics*, Vol. 14, No. 2, 1991, pp. 368–376.

[21]Dorato, P. (ed.), *Robust Control*, Institute of Electrical and Electronics Engineers, New York, 1987.

[22]Dorato, P., and Yedavalli, R. K. (eds.), *Recent Advances in Robust Control*, Inst. of Electrical and Electronics Engineers, New York, 1990.

[23]Mills, R. A., and Bryson, A. E., " Parameter-Robust Control Design Using a Minimax Method," *Journal of Guidance, Control, and Dynamics*, Vol. 15, No. 5, 1992, pp. 1068–1075.

[24]Ray, L. R., and Stengel, R. F., "Stochastic Measures of Performance Robustness in Aircraft Control Systems," *Journal of Guidance, Control, and Dynamics*, Vol. 15, No. 6, 1992, pp. 1381–1387.

[25]Vinh, N. X., Busemann, A., and Culp, R. D., *Hypersonic and Planetary Entry Flight Mechanics*, Univ. of Michigan Press, Ann Arbor, MI, 1980.

[26]Walberg, G. D., "A Survey of Aeroassisted Trajectories," *Journal of Spacecraft and Rockets*, Vol. 22, No. 1, 1985, pp. 3–18.

[27]Mease, K. D. "Optimization of Aeroassisted Orbital Transfer: Current Status," *Journal of the Astronautical Sciences*, Vol. 36, No. 1/2, 1988, pp. 7–33.

[28]Kliore, A. (ed.), *The Mars Reference Atmosphere*, Pergamon, Oxford, 1982.

[29]Box, M. J., "A New Method of Constrained Optimization and a Comparison with Other Methods," *Computer Journal*, Vol. 8, 1965, pp. 42–52.

[30]Kuester, J. L., and Mize, J. H., *Optimization Techniques with FORTRAN*, McGraw-Hill, New York, 1973.

[31]Burden, R. L., Faires, J. D., and Reynolds, A. C., *Numerical Analysis*, Prindle, Weber, and Schmidt, Boston, 1978.

[32]Bate, R. R., Mueller, D. D., and White, J. E., *Fundamentals of Astrodynamics*, Dover, New York, 1971.

[33]Griffin, M. D., and French, J. R., *Space Vehicle Design*, AIAA, Washington, DC, 1991.